

6. Discussion of Results

6.1 Fresh Concrete Test Results

6.1.1 Temperature: Fresh Concrete and Semi-Adiabatic Calorimetry

Temperatures of the fresh concrete varied greatly, as shown in Tables 4-6. Although the concrete mixing was performed in the basement of the Benedict Lab at Michigan Tech, seasonal temperature variation was an issue. During the summer months when the lab was not being heated, the temperature in the lab was strongly influenced by the outside temperature. The variation in fresh concrete temperature is also reflected in the calorimetry plots of Figures 14-17, where some heat curves exhibit an overall elevation relative to others that is assumed to be related, in part, to the ambient temperature in the lab. Of course, the heat evolved over time is also a function of the CMC, the absence/presence of SCMs, as well as the SCM type and replacement level. The most interesting features of the calorimetry plots were the heat curves for the SYN-SLG-6SK-45WC mixtures (i.e. 564 lbs/yd³ CMC 0.45 *w/cm* mixtures containing slag cement, water reducing admixture, and synthetic AEA). These mixtures exhibited a delayed peak in the heat curve relative to the other mixtures as previously discussed in Section 5.1.3. The delayed set of these mixtures, which is associated with the observed delayed peak in the heat curve, was unusual. The LO-SYN-SLG-6SK-45WC concrete mixture was later repeated at various temperature regimes, and with increased dosages of water reducer, but the same delayed-set phenomenon could not be duplicated, as shown in Figures 18 and 19. Further discussion of the delayed-set mixtures is reserved for Section 6.4.

6.1.2 Slump

Figures 8-12 show variation in slump for the different mixtures. As expected, low air content target mixtures consistently yielded lower slumps as compared to their high air content target mixture counterparts. A comparison of Phase II 564 lbs/yd³ CMC mixtures at a *w/cm* of 0.45 and 0.50 shows the expected trend of higher slump for the 0.50 *w/cm* mixtures as shown in Figures 8 and 10. A comparison of Phase II 546 and 470 lbs/yd³ CMC mixtures at a constant *w/cm* of 0.45 shows the expected trend of lower slump for the 470 lbs/yd³ CMC mixtures as illustrated in Figures 8 and 9. The same trend is evident for the Phase III 546 and 490 lbs/yd³ CMC mixtures of Figure 12. As shown in Figure 9, some low air content target mixtures at the 470 lbs/yd³ CMC level exhibited zero slump. Poor consolidation was an issue for these zero slump mixes, and the effects of poor consolidation carried over into some hardened concrete tests; specifically compressive strength and absorptivity as will be discussed later in Sections 6.2.1 and 6.2.2. Contrary to general expectations, the Phase II 0.52 *w/cm* mixtures did not show higher slumps than the 0.50 *w/cm* mixtures, as shown in Figures 10 and 11; this was because the CMC of the 0.52 *w/cm* mixtures was much lower than that of the 0.50 *w/cm* mixtures (517 lbs/yd³ versus 564 lbs/yd³).

6.1.3 Air Content

As can be seen in Figure 13, the air contents as measured by the pressure meter for the concrete mixtures agree well with the target air contents. For the Phase II mixtures prepared at the high air content level, 79.4% were within the specified target range, and 100% were within 3 standard deviations of the target air content. At the low air content level, 85.3% were within the specified target range, and 94.1% were within 3 standard deviations of the target air content. For the Phase III very low air content mixtures, only 50.0% were within the specified target range, but 91.7% were within 3 standard deviations of the target air content. Since measurement of air content spans both fresh and hardened concrete testing, further discussion of the air content test results is reserved for Section 6.3.1.

6.1.4 Water Content and w/cm Testing

Figure 75 compares the water content as measured by microwave oven drying, and the water content (water + admixtures) according to the mixture designs. To run the test, a sample of fresh concrete is weighed and dried to a constant weight ($\Delta\text{mass} < 1\text{g}$) in the microwave oven. According to AASHTO T 318 the water content (expressed in wt. %) is calculated according to Equation 6.1:

$$W_c = 100 \times \left[\frac{W_f - W_d}{W_f} \right] \quad \text{Equation 6.1}$$

Where:

W_c = water content (wt. %)

W_f = weight of fresh concrete

W_d = weight of microwave oven dried concrete

The total water content of the mixture (in terms of lbs/yd^3) is calculated using the concrete unit weight as determined by ASTM C138 according to Equation 6.2:

$$W_T = \frac{(W_c \times U_w \times 27)}{100} \quad \text{Equation 6.2}$$

Where:

W_T = water content (lbs/yd^3)

U_w = unit weight of concrete (lbs/ft^3)

However, Equation 6.1 does not take into account the loss of water absorbed by the aggregate. By convention, water absorbed by the aggregate is not considered part of the water content of the concrete mixture. If the aggregate has considerable moisture content, then Equation 6.1 will overestimate the mixture design water content. With this in mind, Equation 6.3 was developed to account for aggregate absorption:

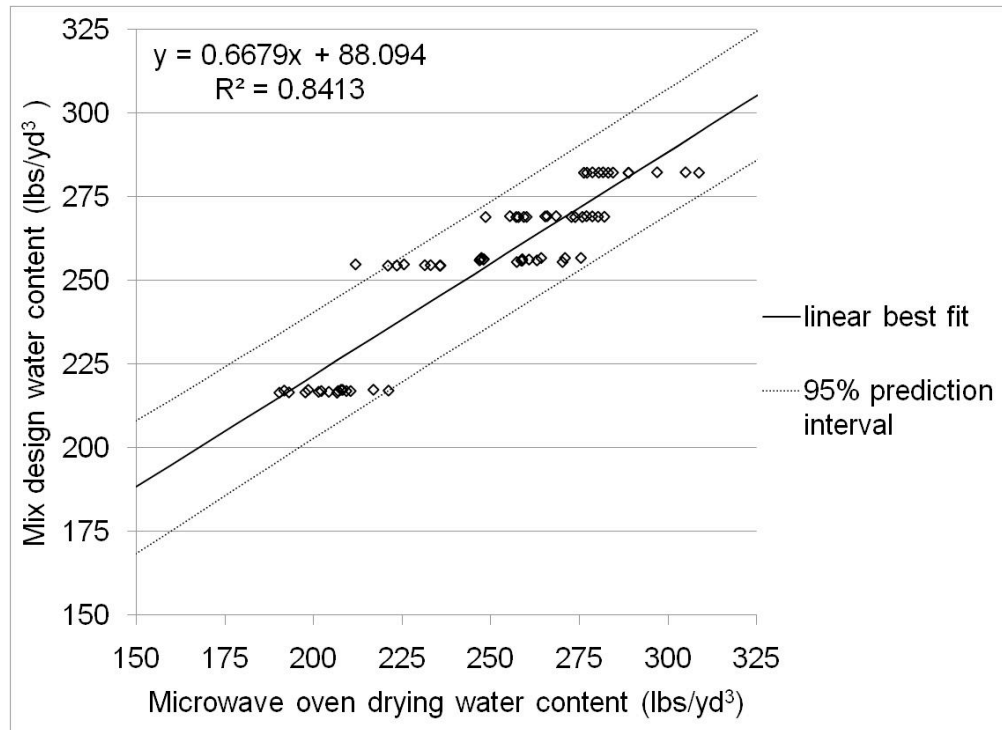


Figure 75: Microwave oven drying test water content results versus mix design.

$$W_c = 100 \times \left[\frac{W_f - W_d}{W_f} \right] - \left[\frac{(C_{abs} \times C_w) + (F_{abs} \times F_w)}{U_w \times V} \right] \quad \text{Equation 6.3}$$

Where:

C_{abs} = absorption value of coarse aggregate (wt. %)

C_w = batch weight of coarse aggregate (lbs)

F_{abs} = absorption value of fine aggregate (%)

F_w = batch weight of fine aggregate (lbs)

V = batch volume (ft³)

The water content values calculated according to Equation 6.3 are listed in Tables 4 and 5, and were also used to create the plot of Figure 75. As shown in Figure 75, the microwave oven drying test tended to overestimate the mixture design water content at low water contents, and underestimate the mixture design water content at higher water contents.

Figure 76 compares the w/cm values as measured by the Cementometer™ using the default factory calibration to the mixture design w/cm values. The Cementometer™ measures the dielectric constant of fresh concrete, and correlates it to w/cm . As shown in Figure 76, the values reported for w/cm are within the correct range for the mixture designs (between 0.35 and 0.55) but there is little correlation to the actual design w/cm values. The w/cm values determined

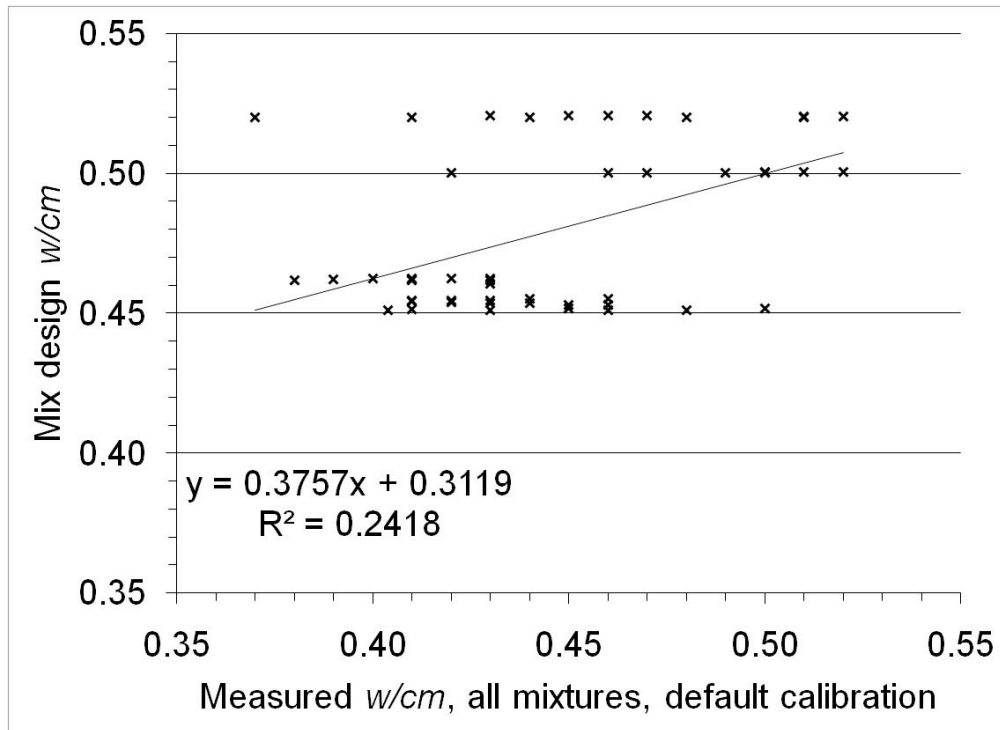


Figure 76: *w/cm* values as measured by the Cementometer™ using the default factory calibration plotted against mixture design *w/cm* values.

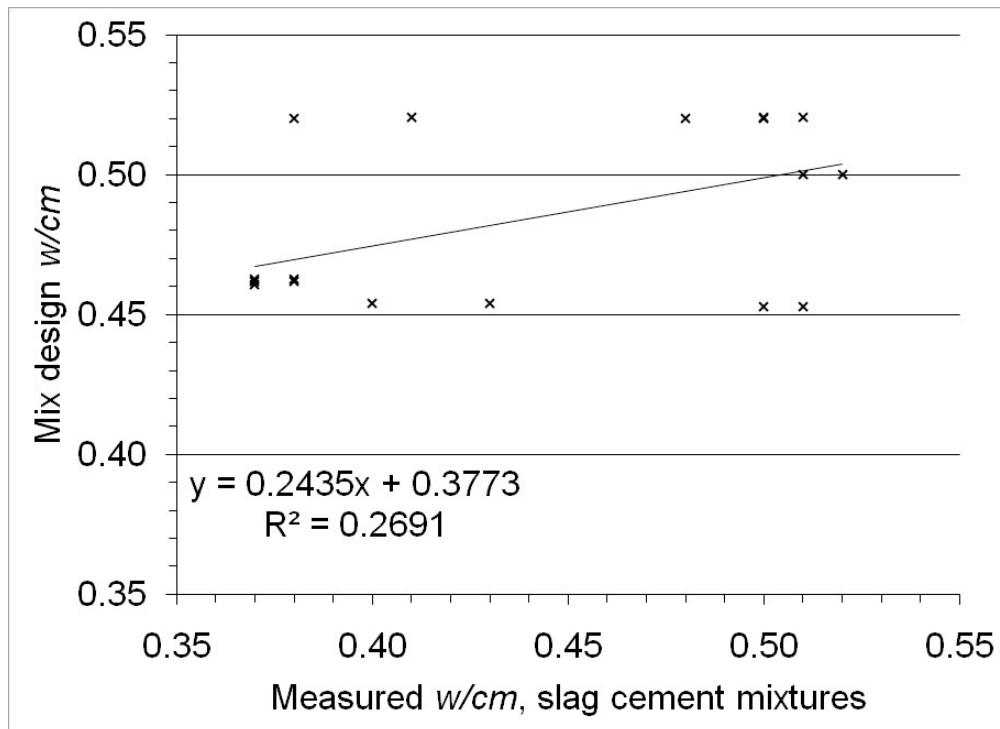


Figure 77: *w/cm* values for slag cement mixtures as measured by the Cementometer™ using in-house calibration plotted against mixture design *w/cm* values.

using the default factory calibration for Type I cement are listed in Tables 4 and 5. The Cementometer™ test was performed immediately upon initial discharge of the fresh concrete mixture into a five gallon plastic bucket. As listed in Tables 4 and 5, there were a few instances where the Cementometer™ test was unintentionally omitted. It should be noted that although the Cementometer™ has a built-in calibration that according to the manual was developed “using every standard and reference available to accurately correlate a relationship between the reading of the probe and that of Type I cement” the manufacturer further advises that the Cementometer™ be calibrated using concrete mixtures that contain aggregate and cementitious combinations commonly encountered by the user. Calibration is accomplished by developing a 0.35 *w/cm* mixture in the laboratory, performing the Cementometer™ test on a sample, then returning the sample to the concrete mixer along with the addition of enough water to raise the *w/cm* by 0.05. After addition of the water, the concrete is thoroughly mixed, and the process repeated until a *w/cm* of 0.75 is obtained. A calibration was performed in-house only for the slag cement mixtures. Figure 77 compares the *w/cm* values of slag cement mixtures as measured by the Cementometer™ using the in-house calibration to the mixture design *w/cm* values. Again, there was little correlation between the measured and mixture design *w/cm* values. Therefore, based on this study, the Cementometer™ does not produce results that correlate with known mixture designs.

6.2 Hardened Concrete Test Results

6.2.1 Compressive Strength and Maturity

As listed in Tables 7-9, and shown in Figures 20-24, all concrete mixtures produced exceeded the recommended minimum design strengths for MDOT Grade P1 concrete pavement mixtures at 7, 14 and 28 days (2,600 psi, 3,000 psi, and 3,500 psi respectively). However, as pointed out in previously Sections 5.1.3 and 6.1.1, the SYN-SLG-6SK-45WC mixtures experienced delayed set, so compressive strength tests could not be performed at 1 and 3 days, as shown in Figure 20. Furthermore, the strength curve from the low air content mixture (LO-SYN-SLG-6SK-45WC) exhibited unusual behavior between 7 and 28 days with unexplained increases and decreases in strength that were inconsistent between the duplicate mixtures. The unusually high strength of 7,128 psi at 7 days for the first LO-SYN-SLG-6SK-45WC mixture coupled with lower strengths of 4,915 and 5,486 psi at 14 and 28 days, respectively, resulted in a negative slope and unusually high intercept for the maturity curve, as reported in Table 12. The maturity curve data for all mixtures are summarized in Tables 11 and 12.

As reported in Section 6.1.2, some 470 lbs/yd³ CMC mixtures were harsh and difficult to consolidate and measured zero slump. The effect of poor consolidation carried over into a few compressive strength test results, specifically for mixtures LO-SYN-PC-5SK-45WC and LO-SYN-SLG-5SK-45WC. What appear to be reductions in compressive strength in Table 8 and Figure 20 can be attributed to the poor consolidation of test cylinders. Cylinders pulled for early age testing from batches that exhibited poor consolidation were selected based on the degree of

observed consolidation issues: cylinders with fewer consolidation problems were tested first, cylinders with more pronounced consolidation issues were tested later.

6.2.2 Absorptivity

The test results for absorptivity listed in Tables 7-9 and Figures 25-29 did not show very consistent trends between different mixtures, although a direct comparison between plots for the straight portland cement mixtures and their slag cement counterparts seems to suggest a tendency towards lower absorptivities in the slag cement mixtures. The unusually high absorptivity curve in Figure 26 for the first LO-SYN-PC-5SK-45WC mixture was likely related to water uptake into large voids present due to poor consolidation. Absorptivity test results as related to F-T durability are discussed further in Section 6.3.3.

6.2.3 Epifluorescent Determination of Equivalent w/cm

Figure 78 compares the measured equivalent w/cm values, as defined in section 5.2.4, to the mix design w/cm values for the vinsol resin AEA concrete mixtures. Figure 79 compares the measured equivalent w/cm values to the mix design w/cm values for the synthetic AEA concrete mixtures. Figures 78 and 79 do show a trend of increasing w/cm with increasing paste fluorescence, however, there is considerable scatter, and also a tendency towards the underestimation of the mix design w/cm . The underestimation could be partially explained by the fact that the mortar standards were moist cured for only 28 days, while the concrete mixtures were moist cured for 120 days, allowing for more time for hydration products to form, resulting in a denser capillary pore structure. Figures 78 and 79 also show a wide scatter for the individual measurements, with a 95% prediction interval on the order of ± 0.05 for equivalent w/cm .

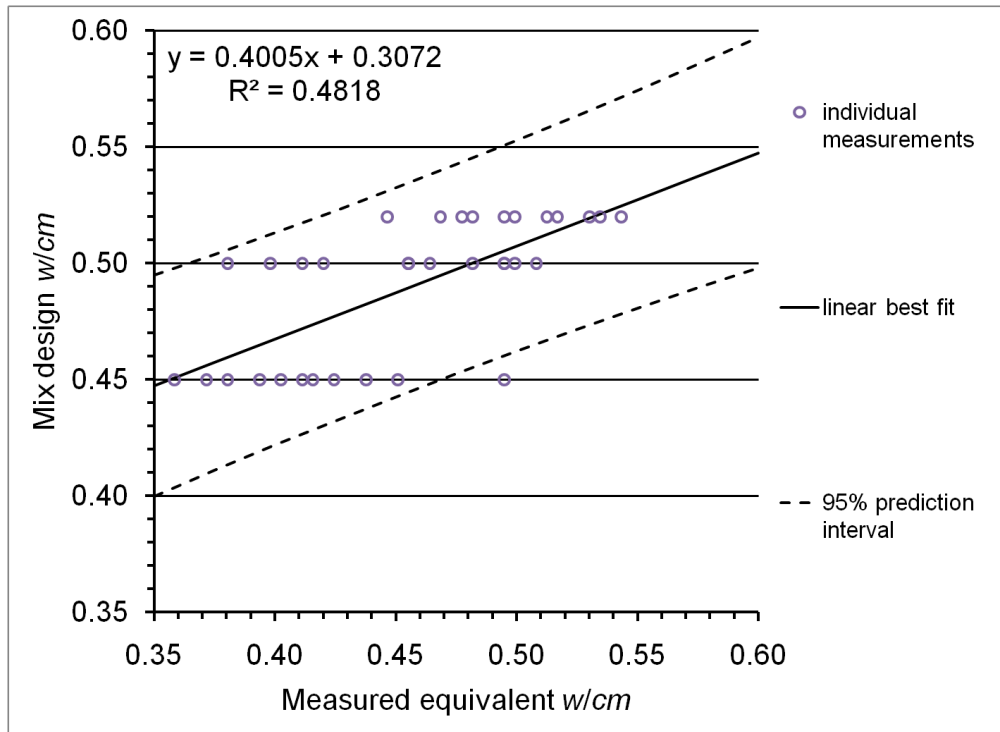


Figure 78: Equivalent w/cm values for vinsol resin AEA portland cement concrete mixtures as measured by paste fluorescence plotted against mixture design w/cm values.

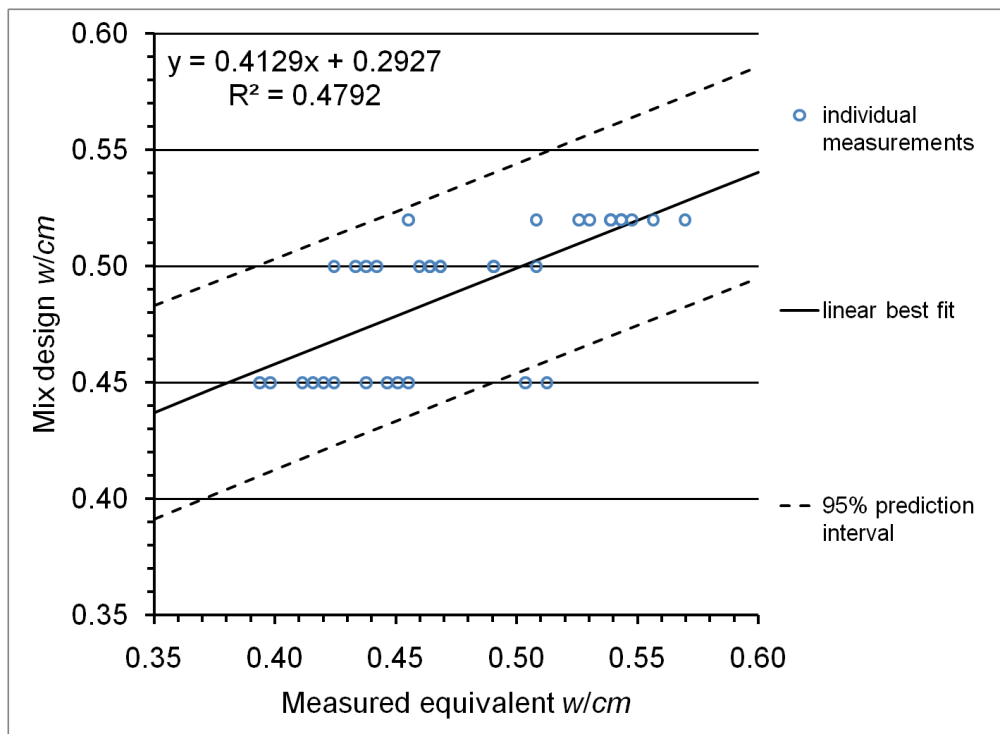


Figure 79: Equivalent w/cm values for synthetic AEA portland cement concrete mixtures as measured by paste fluorescence plotted against mixture design w/cm values.

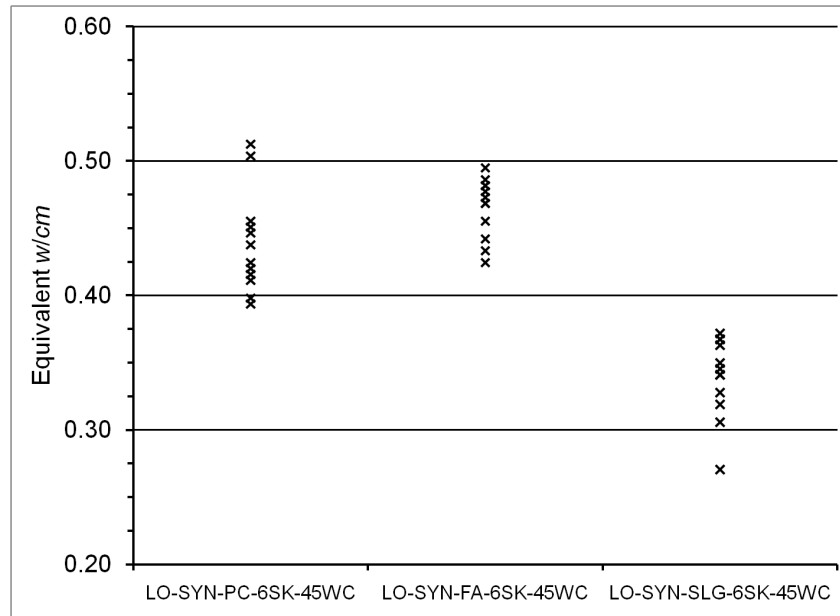


Figure 80: Equivalent w/cm measurements from concrete mixtures made with w/cm of 0.45, both with and without SCMs.

To show the influence of SCM content, Figure 80 plots the measured equivalent w/cm ratios from the 100% portland cement, the 25 wt. % replacement fly ash, and the 40 wt. % replacement slag cement concrete mixtures. As shown in Figure 80, the equivalent w/cm values measured from the slag cement concrete mixture are significantly lower than those of the portland cement mixture, reflecting a denser cement paste microstructure, while the equivalent w/cm values measured from the fly ash mixture are slightly higher than the portland cement mixture.

The conversion of fluorescence measurements collected from concrete made with varying SCM contents, and varying cure times, to equivalent w/cm values derived from calibration curves developed from fluorescence measurements collected from 28-day moist cured mortar standards produced with 100% portland cement introduces significant complications to the interpretation of the original w/cm of the concrete. Ideally, the standards used to develop the calibration curve should be as similar as possible to the concrete of interest in terms of composition and curing. However, the production of standards for every situation is not practical. At best, the fluorescence method is useful only in terms of determining how the concrete compares to the standards; and is by no means a measurement of the actual w/cm used to produce the concrete.

6.2.4 F-T Testing

As summarized in Tables 7-9 and Figures 30-36, only five mixtures (LO-VR-FA-6SK-45WC, LO-VR-SLG-5SK-45WC, VLO-VR-FA-6SK-46WC, and VLO-SYN-FA-6SK-46WC) exposed to the Procedure B (freeze in air) testing regime failed the ASTM C666 criteria with durability factors that dropped below 60 at or before 300 cycles, although six additional mixtures (LO-SYN-SLG-6SK-45WC, LO-SYN-FA-6SK-45WC, LO-SYN-SLG-5.5SK-52WC, VLO-VR-SLG-6SK-46WC, and VLO-SYN-SLG-6SK-46WC, and VLO-SYN-SLG-5.2SK-46WC) experienced notable drops in relative dynamic modulus of elasticity (RDME).

In addition to the ASTM C666 Procedure B testing, the Phase III very low air content mixtures were also tested under Procedure A (freeze in water) and an alternative to Procedure A where the beams were frozen in a 4.0 wt. % CaCl_2 brine. As summarized in Table 10 and Figures 34-36, the Procedure A test regimes were more aggressive than Procedure B, with a slightly larger fraction of Phase III mixtures experiencing notable drops in RDME (50% as opposed to 42%). Furthermore, the concrete beams tested under the Procedure A regimes exhibited more surface scaling than the companion beams tested under Procedure B, as shown in the weight change plots of Figures 37-39.

As described in Section 5.2.2, a small number of Phase II beams already tested under Procedure B underwent additional F-T cycling under Procedure A, with freezing in water, as well as freezing in 4.0 wt. % CaCl_2 brine and freezing in 4.2 wt. % NaCl brine. The results of the extended F-T testing are summarized in Tables 13 and Figures 40 and 41. The limited population of beams was selected to explore the influence of air content, CMC, and w/cm on F-T durability under the more aggressive Procedure A protocols. All beams made from concrete mixtures with a w/cm of 0.50 and 0.52 rapidly failed, although measurements of RDME were problematic, with severe scaling and mass loss interfering with the measurements of resonant frequency. The high air content 0.45 w/cm mixtures fared better, with negligible drops in RDME, but scaling was more pronounced in beams from the 564 lb/yd^3 CMC mixtures than from the 470 lb/yd^3 CMC mixtures. Low air content 0.45 w/cm beams also exhibited pronounced scaling at both CMC contents, but only beams from the 564 lb/yd^3 CMC mixtures showed considerable reductions in RDME. Further discussion of the ASTM C666 Procedure B test results is continued in the following section.

6.3 F-T Performance Related to Other Parameters

6.3.1 Air-void Parameters and F-T Performance

Figure 81 illustrates the range of results that were obtained for total air content when using the common methods of measuring fresh air content (i.e. ASM C231, ASTM C173, and ASTM C138) and methods of determining the complete air-void system parameters (i.e. flatbed scanner and the AVA). As seen in Figure 81a, the pressure meter and volumetric meter are in good agreement, and are dependable methods of measuring total air content. However, these methods only provide a measure of air content while other air-void parameters are also important in predicting F-T performance. Figure 81b compares the results of air content determined by gravimetric methods to the pressure meter results. The gravimetric results correlate well but generally under report the total air content. Figure 81c presents the results of measuring the total air content by the AVA as compared to the results obtained from the pressure meter. The results shown in Figure 81c do not include results that would plot off the scale used (e.g. results of negative air content). Although the AVA air content test results show a poor correlation with the

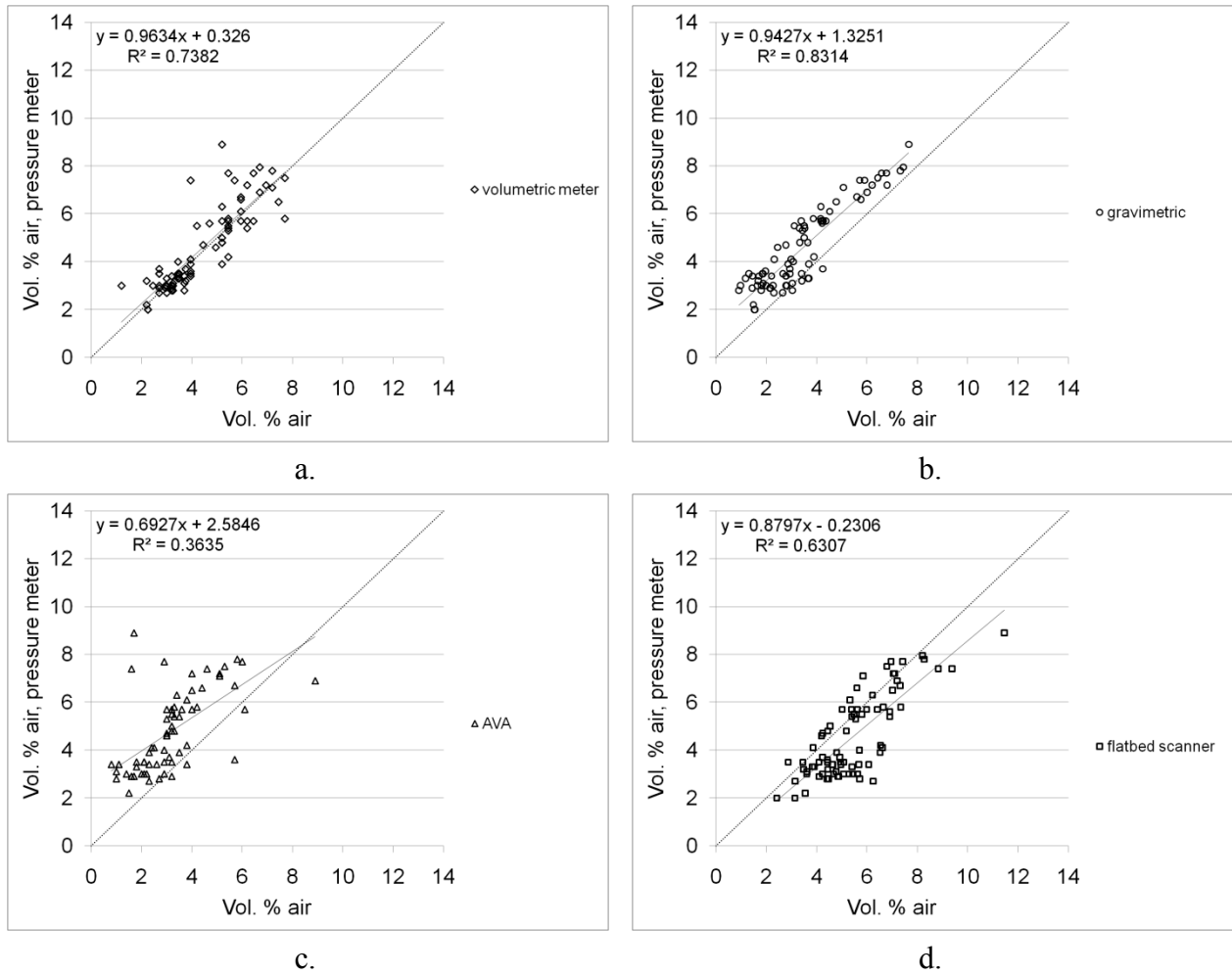


Figure 81: Air content measured by ASTM C173 (volumetric meter) ASTM C138 (gravimetric air) the AVA and flatbed scanner compared to that measured by the pressure meter.

pressure meter test results, it should be noted that the sampling procedure used by the AVA (i.e. a vibrating cage that excludes coarse aggregate to obtain a mortar sample) tends to eliminate large entrapped air-voids that would otherwise be included in a determination of air content by the other methods. Finally, Figure 81d presents the results of analyses performed using a flatbed scanner. The flatbed scanner is not currently an accepted method of performing ASTM C457 but it is under consideration for inclusion in the test method. Figure 81d illustrates that the flatbed scanner method correlates well with the air content measured by the pressure meter but slightly overestimates the total air content. This is due to a combination of effects. First, the resolution of the flatbed scanner image is limited by the $8 \times 8 \mu\text{m}$ pixel dimensions at the scanned resolution of 125 dpm. At this resolution the brightness of pixels near the perimeters of air-voids (as defined by the recesses filled with white powder) is a combination of the black paste and the white air-void. As a result, the edges of the air-voids are not well defined. Second, in the stereomicroscope image, areas within the air-voids are defined by dark shadows, while the perimeters, which are slightly eroded during polishing, appear bright due to the oblique illumination of the microscope lamp. This high contrast between the dark shadows and bright

edges results in well-defined outlines for the entrained air-voids. In the scanned image, the white powder fills not only the deeper portions of the air-voids, but also the eroded regions at the edges, making the air-voids appear slightly larger, as illustrated in Figure 82.

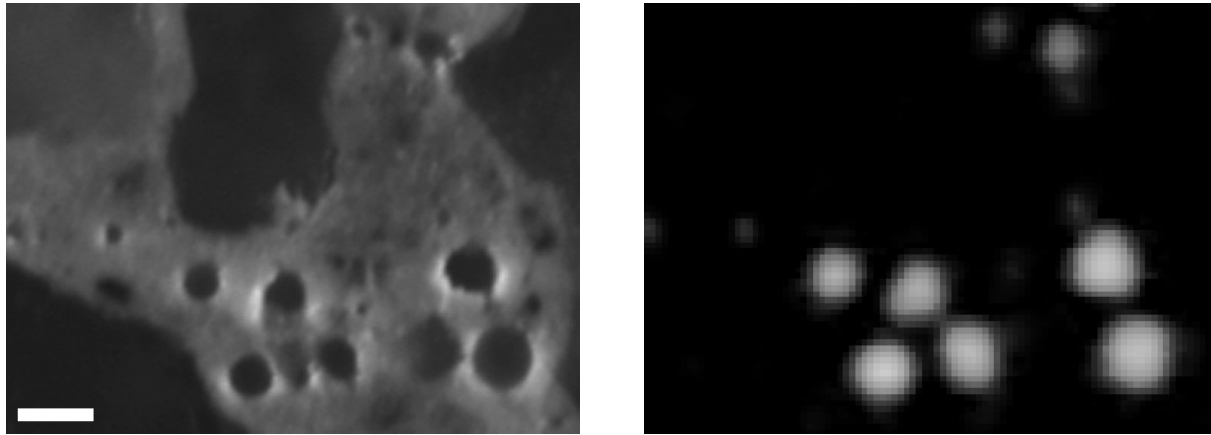


Figure 82: Stereomicroscope image of polished surface enlarged to 100× magnification as per LS-432 specifications (left), and the same area after black and white treatment as-scanned with flatbed scanner at a resolution of 125 dpm (right), white bar = 100 μm .

A third source for the slight overestimation of the total air content involves a compromise to allow the detection of the smallest air voids, but at the expense of artificially overestimating the size of large air voids. In the flatbed scanner method, the total air content is determined by the number of air-pixels in the traverse line divided by the total number of pixels in the traverse line. The void frequency is measured by the number of air-void intercepts with the traverse line divided by the total traverse line length. From these two values and the paste content, the spacing factor is computed, as outlined in ASTM C457. The simplicity of the approach allows for the computation of the air-void parameters for a sample in less than a minute. However, the simplicity of the approach also introduces some problems. Figure 42 compares the influence of threshold level choice on automated air content and void frequency test results as compared to manual test results for the 20 calibration samples. As shown in Figure 42, the difference between the flatbed scanner and manual test results for air content and void frequency achieved minimum values at threshold levels of 115 and 174 respectively. The lower threshold level encourages the detection of smaller entrained air voids, but at the same time effectively dilates the larger air voids, leading to a slight overestimation of air content. Figures 83 and 84 compare the specific surface and spacing factor values reported by the AVA and the flatbed scanner. Although there is little correlation between the methods, when the two parameters are plotted against each other on a method by method basis, as in Figure 85, the expected inverse trends between specific surface, spacing factor, and air content are observed.

The plots of Figure 85 also incorporate ASTM C666 F-T Procedure B test values for durability factor. In examining Figure 85a, the lower limit of the high target air mixtures, in terms of total air content, is consistent with what is commonly considered durable in F-T environments. It is interesting to note the generally accepted threshold of F-T durability, in terms of spacing factor

as measured by the flatbed scanner (i.e. 0.2 mm), agrees very well with the distinction of F-T durable and non-durable concrete as measured by total air content. The results from the AVA would indicate that possibly a higher threshold could be adopted (e.g. 0.3 mm), but using 0.2 mm as the threshold of F-T durability is clearly a more conservative value. Given the concern for accuracy with the AVA, it is not recommended that a threshold of F-T durability be adopted other than 0.2 mm, even if the AVA is used to make that determination.

The same trends seen in Figures 85a and 85b are evident in Figures 85c and 85d. That is, the generally accepted threshold of 0.2 mm for the air-void system spacing factor, as measured by ASTM C457, is an acceptable threshold to delineate F-T durable concrete from non-durable concrete. What can be seen, however, is that a demarcation of 0.2 mm is not an absolute determination of F-T durability as many concrete mixtures with a spacing factor greater than 0.2 mm did not fail the ASTM C666 test. In other words, it is clearly possible to have F-T durable concrete with an air-void system spacing factor greater than 0.2 mm. This is not to argue that the 0.2 mm criteria is irrelevant. Rather, it indicates that the accepted criteria of 0.2 mm is a safe, conservative threshold and any changes in this specification would most likely require coupling the measured spacing factor with some other criteria. It should also be noted that all concrete mixtures that failed the F-T test were prepared with low or very low target air contents.

The volume fraction of cement paste within a specified distance of an air-void, or more generally, the paste-void proximity distribution, provides an alternative means to describe the air-void system in concrete. Methods for computing the paste-void proximity distribution have been summarized by Snyder et al. [2001] and the method described by Philleo [1983] was explored here for comparison to the most commonly used parameter for the prediction for F-T durability, the spacing factor. Figure 86 compares spacing factor values, durability factor values, and volume fractions of cement paste within various distances of an air-void. Figure 86a shows that in all cases, more than 90% of the cement paste was within 0.2 mm of an air-void. Figure 86b shows that when approximately 80% or less of the cement paste was within 0.1 mm of an air-void, concrete mixtures with durability factor values of less than 95 become more prevalent. Similar trends occur at values of 40% for paste within 0.05 mm of an air-void, and 20% for paste within 0.025 mm of an air-void.

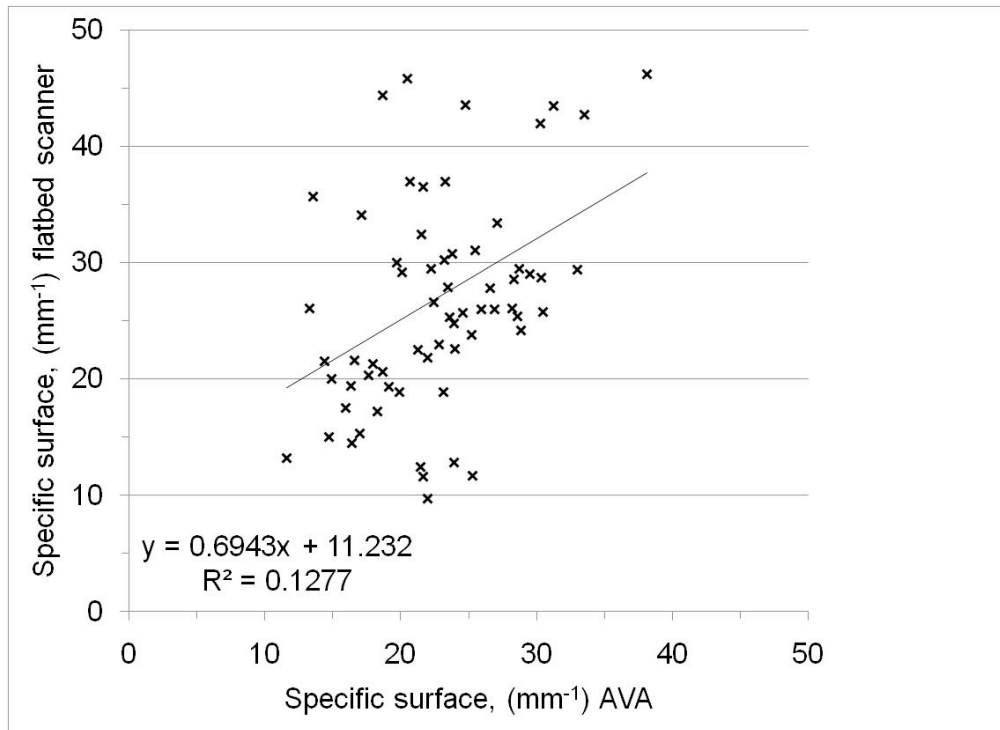


Figure 83: Comparison of specific surface measurements using AVA and flatbed scanner.

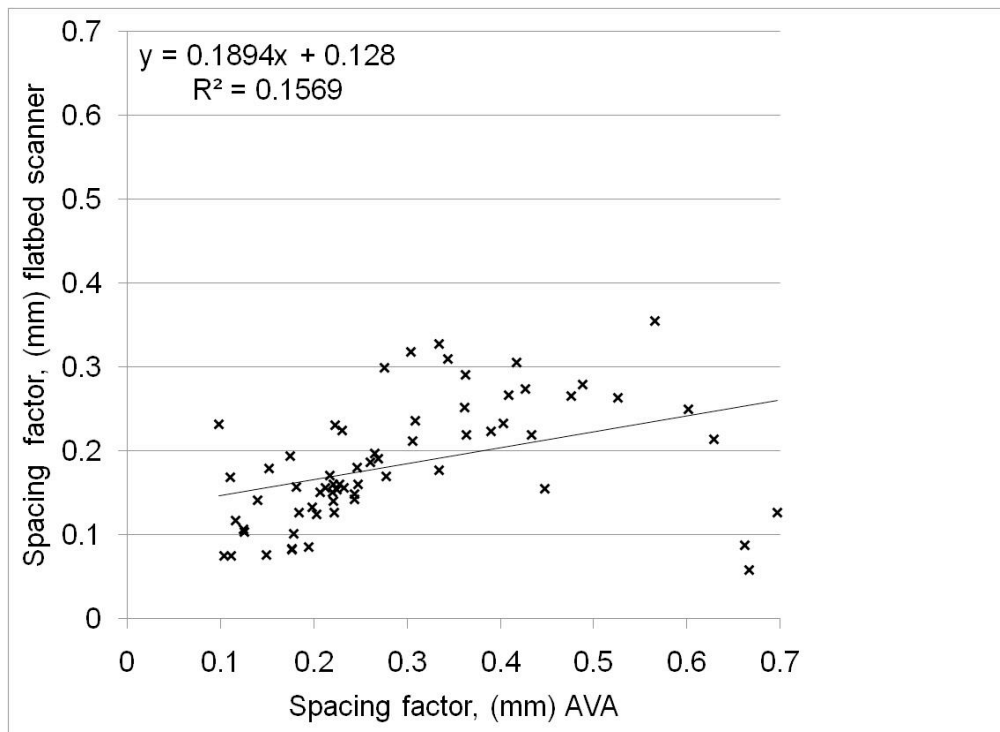
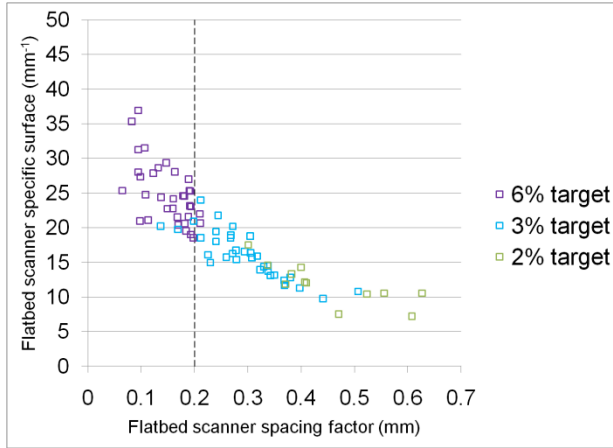
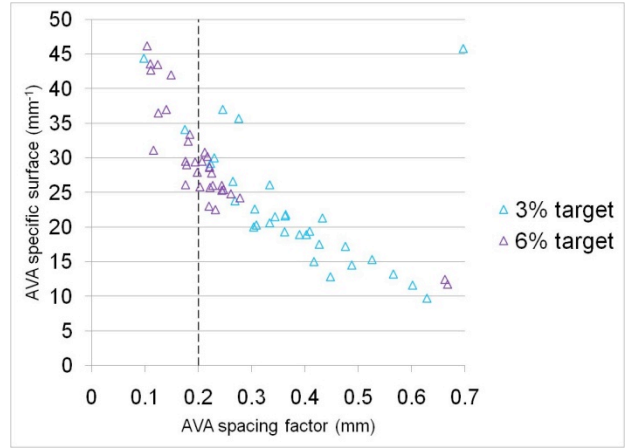


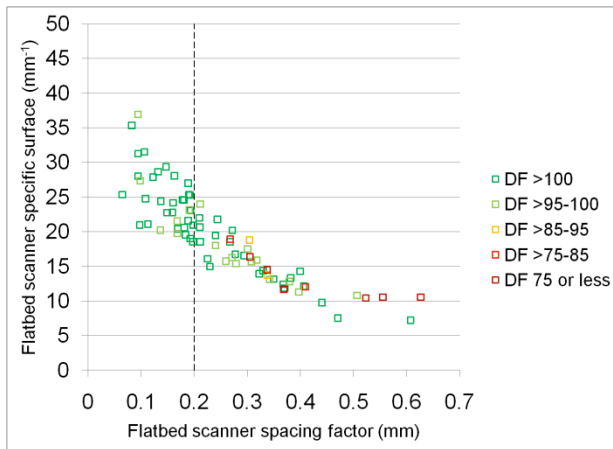
Figure 84: Comparison of spacing factor measurements using AVA and flatbed scanner.



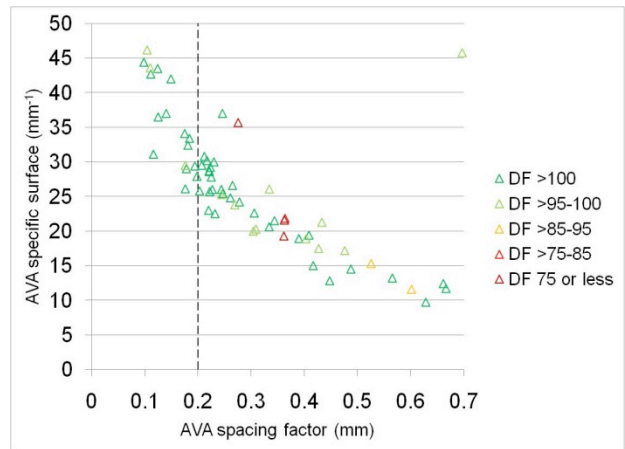
a.



b.



c.



d.

Figure 85: Measured specific surface versus measured spacing factor by flatbed scanner and the AVA. Figures 85a and 85b show the relationship in terms of the target air content and Figures 85c and 85d in terms of DF. Dashed line shows traditional spacing factor threshold at 0.2 mm.

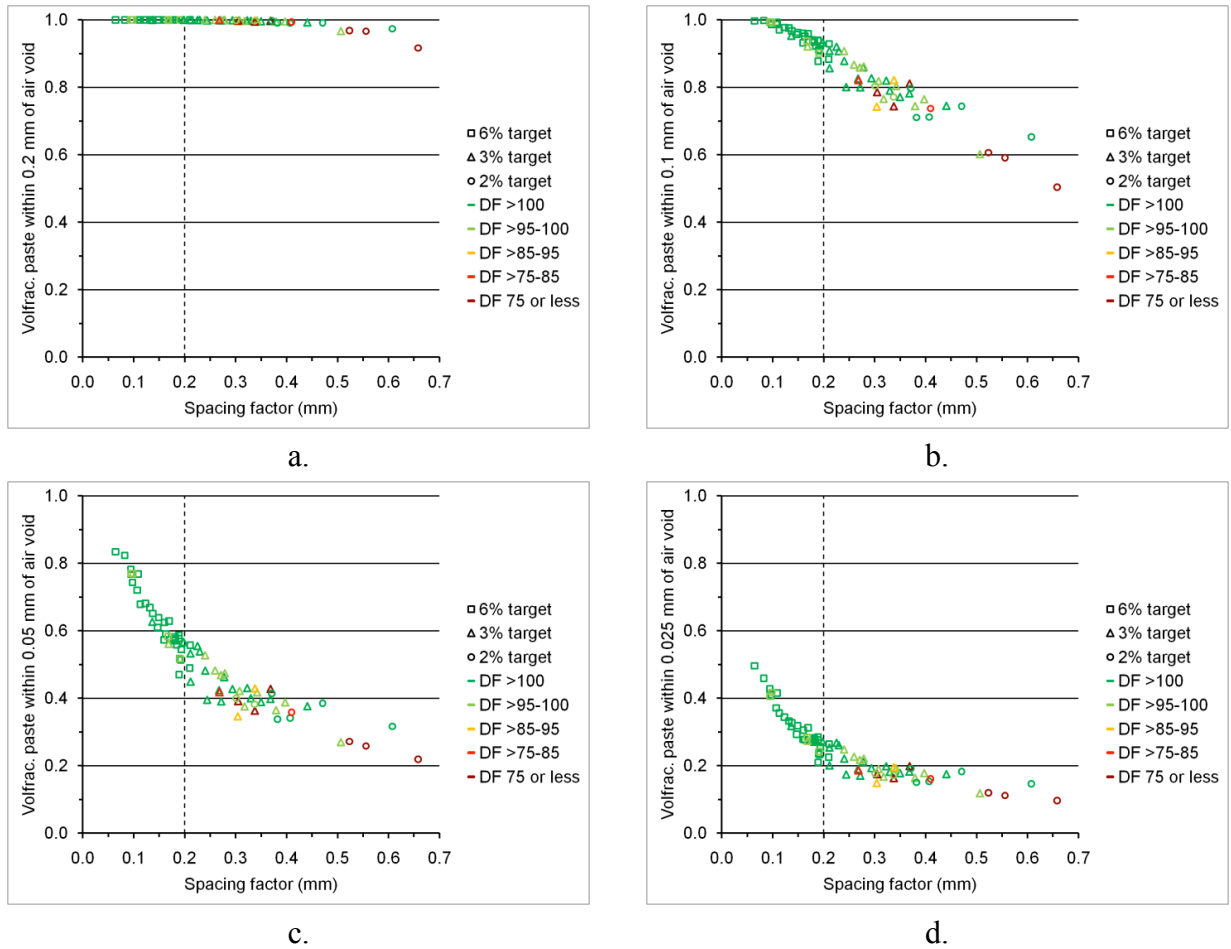


Figure 86: Volume fractions of cement paste within 0.2 mm (a), 0.1 mm (b), 0.05 mm (c), and 0.025 mm of an air-void (d) for all concrete mixtures, plotted against spacing factor, and color-coded in terms of the ASTM C666 durability factor.

Figure 87 plots the Philleo factor against the spacing factor for all concrete mixtures. The Philleo factor is a distance, and represents the maximum distance from a point in the hardened cement paste to an air void for 90% of the hardened cement paste in the concrete. It is simply another method of describing the protected paste volume. Air-void chord length distributions derived from the same images used to compute the spacing factor values were used to compute the Philleo factor. As can be seen in Figure 87, there is a strong correlation between the spacing factor and the Philleo factor, and the Philleo factor performs just as well as the spacing factor in terms of predicting F-T performance. About a quarter, or 24% (11 out of 45) of the concrete mixtures that exceeded the traditional 0.2 mm spacing factor limit exhibited durability factor values less than 95. The predictive performance of the Philleo factor was very similar. For instance, if a line is drawn at a Philleo factor of 0.1 mm, 27% (11 out of 41) of the concrete mixtures exhibited durability factor values less than 95. For this study, even when the spacing factor and Philleo factor limits are pushed to just below the threshold of the poorly-performing FT mixtures (0.25 and 0.11 mm respectively), roughly two-thirds of the concrete mixtures exceeding those values performed well in terms of durability factor.

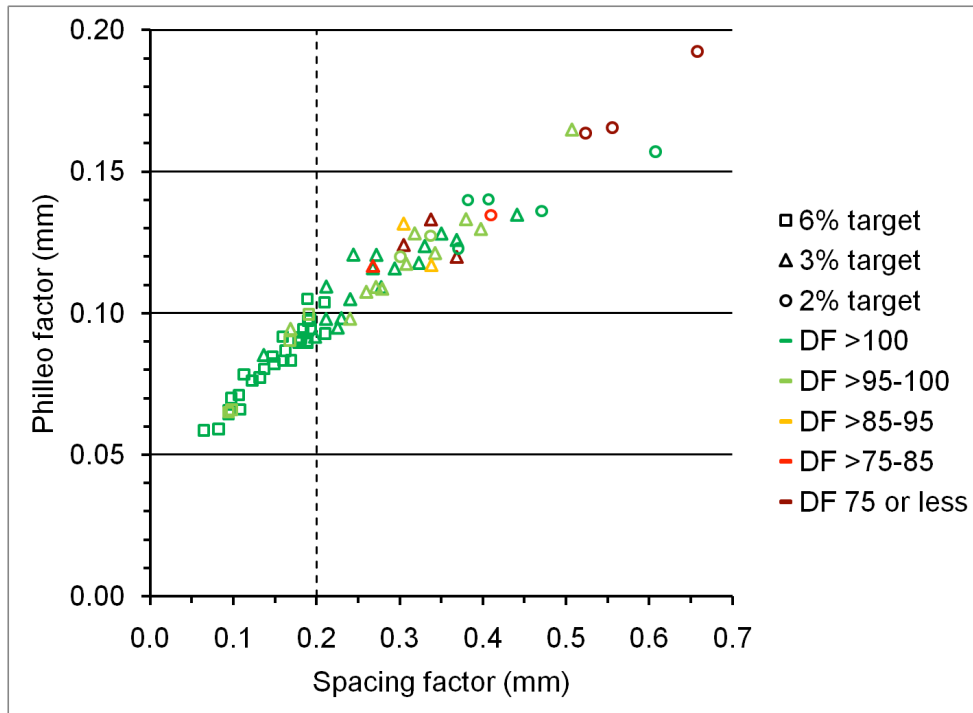


Figure 87: Philleo factor vs. spacing factor for all concrete mixtures, plotted in terms of concrete mixture target air content and ASTM C666 durability factor.

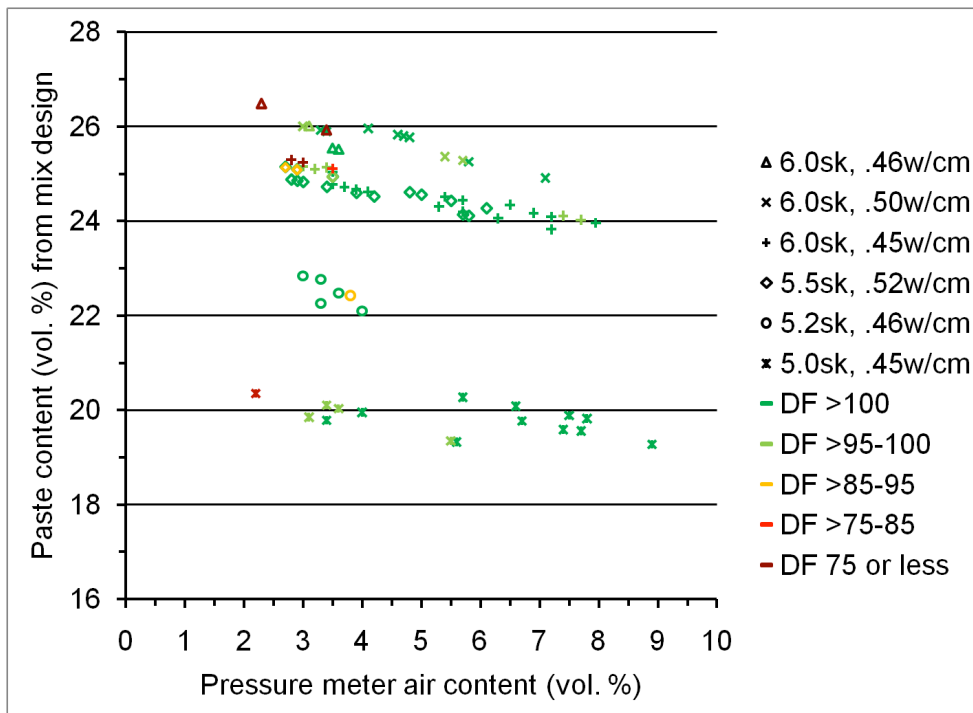


Figure 88: Paste content (total concrete volume minus aggregate and air volumes) vs. pressure meter air content for all concrete mixtures plotted according to durability factor, CMC, and w/cm .

Computation of both the spacing factor and the Philleo factor require measurements of paste content and the air content of the concrete mixture, along with more detailed measurements of the air-voids (i.e. the air-void frequency or the air-void chord length distribution). However, even without detailed air-void measurements, the same F-T durability trends are apparent in a simple plot of paste content vs. air content, as shown in Figure 88. Figure 88 was constructed using the results of the pressure meter test and an estimate of the paste content based on the mix design, as shown in Equation 6.4:

$$p = \frac{-p_c(A - 100)}{p_c + G_c}$$

Equation 6.4

Where:

p = Paste content (vol.%) where paste is defined as the total concrete volume minus the aggregate and air volumes.

A = Air content (vol.%) from pressure meter test.

p_c = Sum of mass of cement divided by specific gravity of cement + mass of SCMs divided by the specific gravity of SCMs + mass of water (including fluid admixtures) divided by the specific gravity of the fluids.

G_c = Sum of the masses of the aggregates, each divided by its specific gravity.

The concrete mixtures from Figure 88 are plotted according to CMC, w/cm , and durability factor. Concrete mixtures with the same CMC and w/cm tend to plot in horizontal linear groupings with slightly negative slopes, since the paste content increases as the air content decreases. As this occurs, the instances of poorly-performing concrete mixtures increase. All concrete mixtures with a total air content less than 2.5 vol. % failed in F-T testing (with failure defined as a durability factor of less than 60 at 300 cycles). The remaining poorly-performing concrete mixtures (those with durability factor values less than 95) all had air contents less than 3.5 vol. % and paste contents greater than 25 vol. %. In this category 39% (7 out of 18) of the concrete mixtures performed poorly in terms of F-T durability under ASTM C666 Procedure B testing (i.e. freezing in air).

As part of the flatbed scanner analysis, air-void chord length distributions were collected. Figure 89 plots the air-void chord length distributions of the concrete mixtures, grouped according to their target air contents, and according to their ASTM C666 Procedure B durability factor values. For all mixtures, a peak in void frequency occurs for chord lengths within the range of 30 to 40 μm . When the frequency of chord lengths within this range drops below 0.01 voids/mm the incidence of poorly-performing concrete mixtures increases.

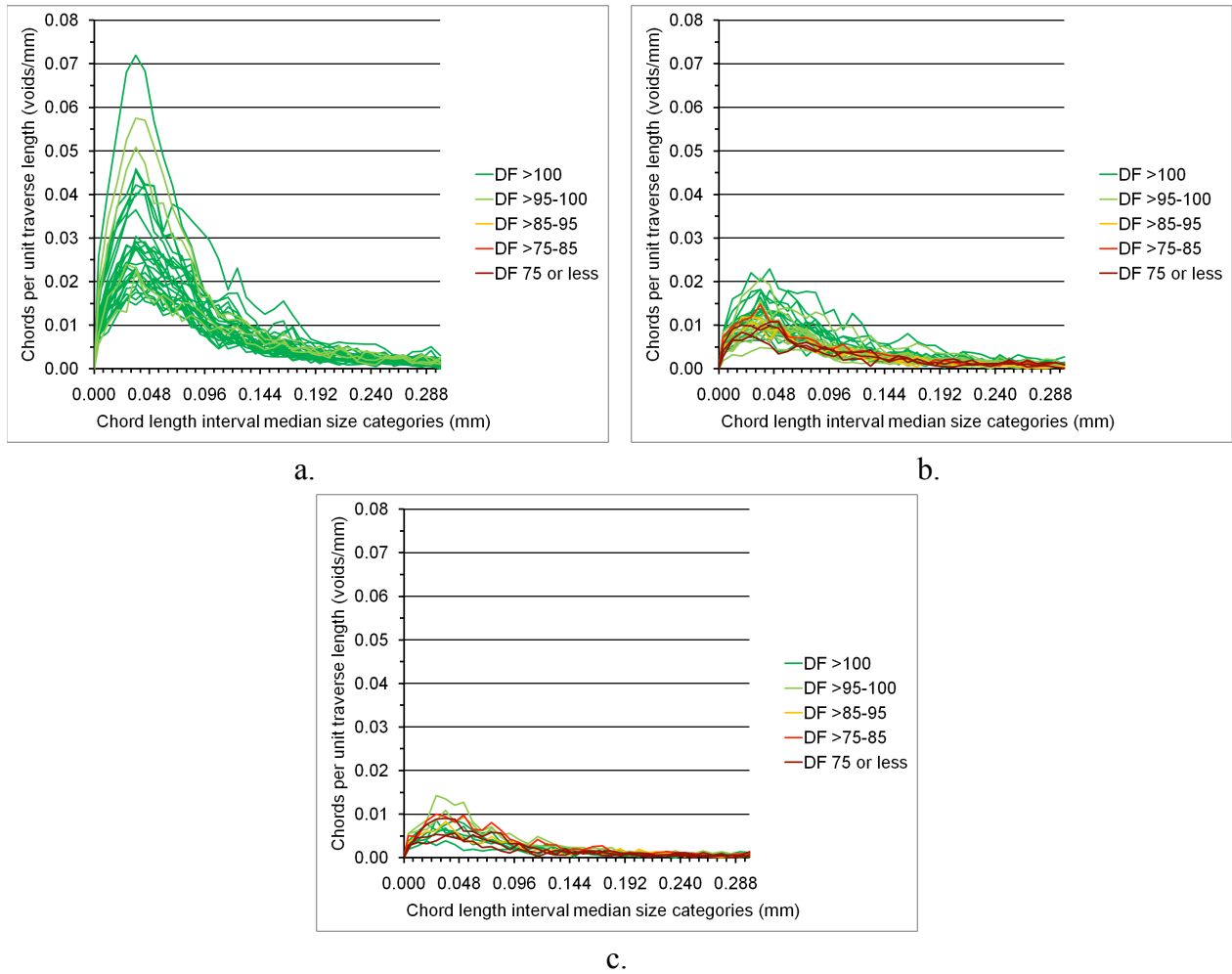


Figure 89: Chord length size distribution plots color-coded in terms of durability factor for (a) high target air content mixtures, (b) low air content target mixtures, and (c) very low air content target mixtures.

6.3.2 SCM Replacement and F-T Performance

Considering the matrix of concrete mixtures prepared for this study, a key point is the role of SCM replacement on the demonstrated F-T performance. Most concrete mixtures currently being used have some level of SCM replacement and there is concern amongst some state highway agencies that these SCM replacements might compromise F-T performance. To address this concern it is important to first look at the conventional measures of performance (i.e. the spacing factor) and then examine the actual performance achieved.

The first two rows of Table 29 present the breakdown of which concrete mixtures would be considered durable or non-durable with respect to F-T damage, on the basis of an evaluation of the air-void system parameters. Based upon this conventional measure, the majority of low and very low target air mixtures would be rejected. As seen in the last row of Table 29, only a small portion of the concrete mixtures received a durability factor of less than 85 during the ASTM

C666 Procedure B testing (only 8 out of 46, or 18.6%). However, of those mixtures that failed, all contained either fly ash or slag. But, factors other than SCM content may also have

Table 29: Summary of how the low and very low target air mixtures would be classified for F-T durability based upon ASTM C457 results, and also a summary of how many low and very low target air mixtures actually failed ASTM C666 testing with a durability factor less than 85 at 300 cycles.

Classification	Supplementary Cementitious Material		
	<i>None</i>	<i>Fly Ash</i>	<i>Slag</i>
Durable (Spacing Factor < 0.2 mm)	15.0% (3/20)	0.0% (0/8)	0.0% (0/18)
Non-durable (Spacing Factor > 0.2 mm)	85.0% (17/20)	100.0% (8/8)	100.0% (18/18)
Non-durable - Durability Factor < 85	0.0% (0/20)	62.5% (5/8)	16.7% (3/18)

come into play. The majority of concrete mixtures with durability factors less than 85 had a CMC of 564 lbs/yd³, with the exception of the single poorly consolidated mixture with a CMC of 470 lbs/yd³ (LO-VR-SLG-5SK-45WC). As previously discussed in 6.3.1, and illustrated in Figure 88, the air content and paste content were indicative of F-T performance; mixtures with low air contents and high paste contents had the highest rates of failure. Figures 90 and 91 plot the air contents and paste contents from all 564 lbs/yd³ CMC mixtures made at a *w/cm* of 0.45 or 0.46 in terms of both SCM content and durability factor. For the low and very low target air concrete mixtures, those with fly ash had both the lowest air contents and the highest paste contents. Paste content, defined here as the total concrete volume minus the aggregate and air volumes, will naturally increase as the air decreases. So, it is not surprising that the low air content fly ash mixtures also have the highest paste contents. At a constant CMC, it is true that the paste volume of mixtures containing SCMs will be slightly higher than their 100% portland cement counterparts, since the specific gravities of SCMs are lower than that of portland cement. However, this increase in volume is on the order of less than one percent when calculated in terms of the total volume of the concrete, and is insignificant as compared to the influence of total air content. The other important consideration is the impact of fly ash on air entrainment as a result of adsorption of AEA onto carbon particles in the fly ash, thereby impacting air entrainment. However, this issue was not a part of this study.

In summary, all SCM mixtures made at the high target air content performed well, but at the same time, roughly a third of the low and very low target air SCM mixtures (8 out of 26, or 30.8%) had durability factors of less than 85. Whether this performance record is due to the presence of SCMs, the entrained air-void systems, or a combination both is difficult to determine.

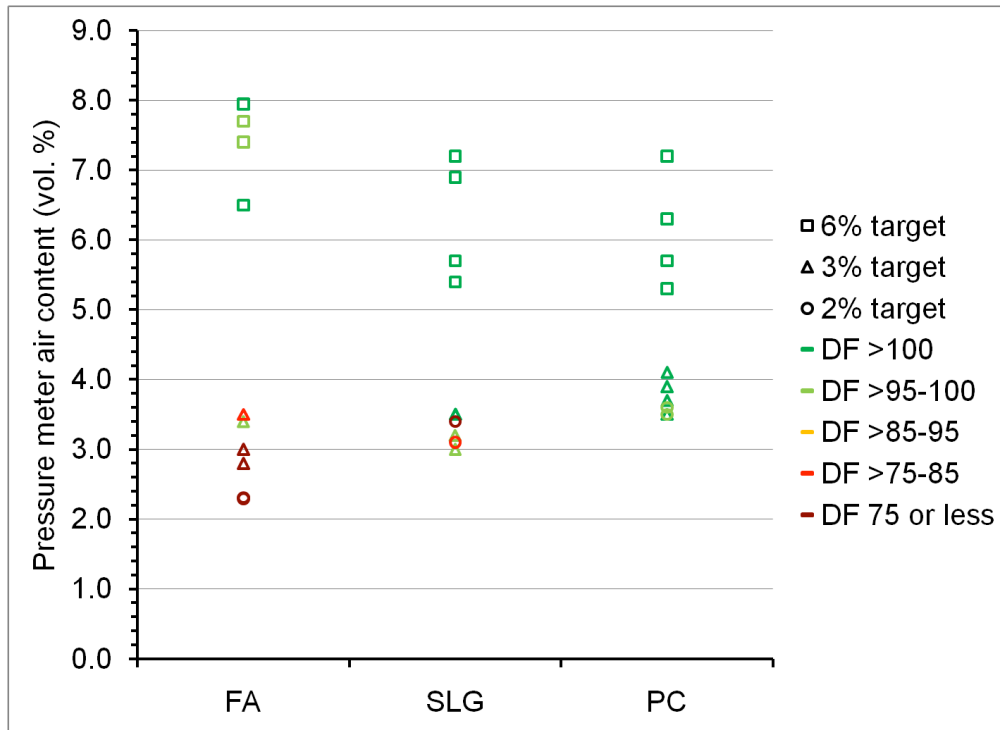


Figure 90: Air content measurements for the 564 lbs/yd³ CMC mixtures made at a *w/cm* of 0.45 and 0.46, plotted in terms of durability factor and SCM content.

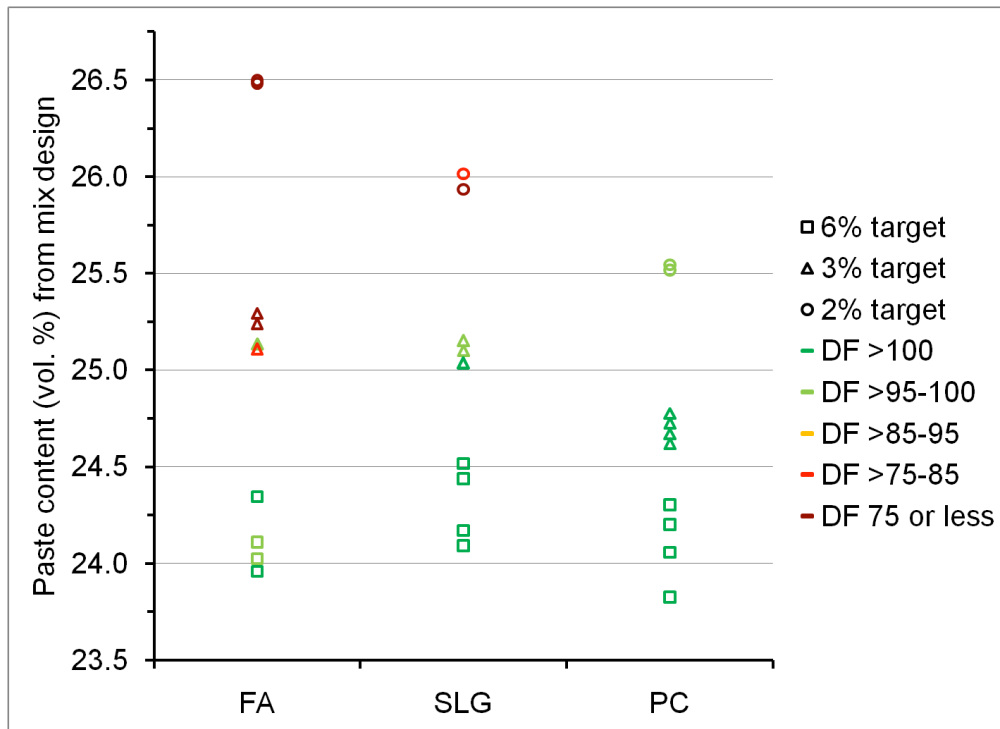


Figure 91: Paste content (total concrete volume minus aggregate and air volumes) for the 564 lbs/yd³ CMC mixtures made at a *w/cm* of 0.45 and 0.46, plotted in terms of durability factor and SCM content.

6.3.3 Absorptivity and F-T Performance

Figure 92 plots the absorptivity curves of the concrete mixtures, grouped according to their target air contents, and according to their ASTM C666 Procedure B durability factor values. At the end of Phase II, the plot shown in Figure 92b suggested an apparent “pessimism” absorptivity leading to F-T damage. At low absorptivity, the degree of saturation appeared low enough to prevent damage from freezing and thawing. At high absorptivity, the water appeared able to move more freely through the capillary pore system and again, F-T damage is avoided. In the pessimism range of absorptivity, it appeared that perhaps water was able to penetrate and saturate, but not readily flow through the concrete, thereby causing F-T damage. However, after the completion of the Phase III mixtures, as shown in Figure 92c, the same pattern no longer held, with the lowest absorptivity concrete mixtures performing poorly in F-T. Furthermore, the drastically lower and very consistent absorptivity values for the Phase III mixtures was in sharp contrast to the wide spread of absorptivity values from the Phase II mixtures, making it difficult to draw any inferences overall from the absorptivity data.

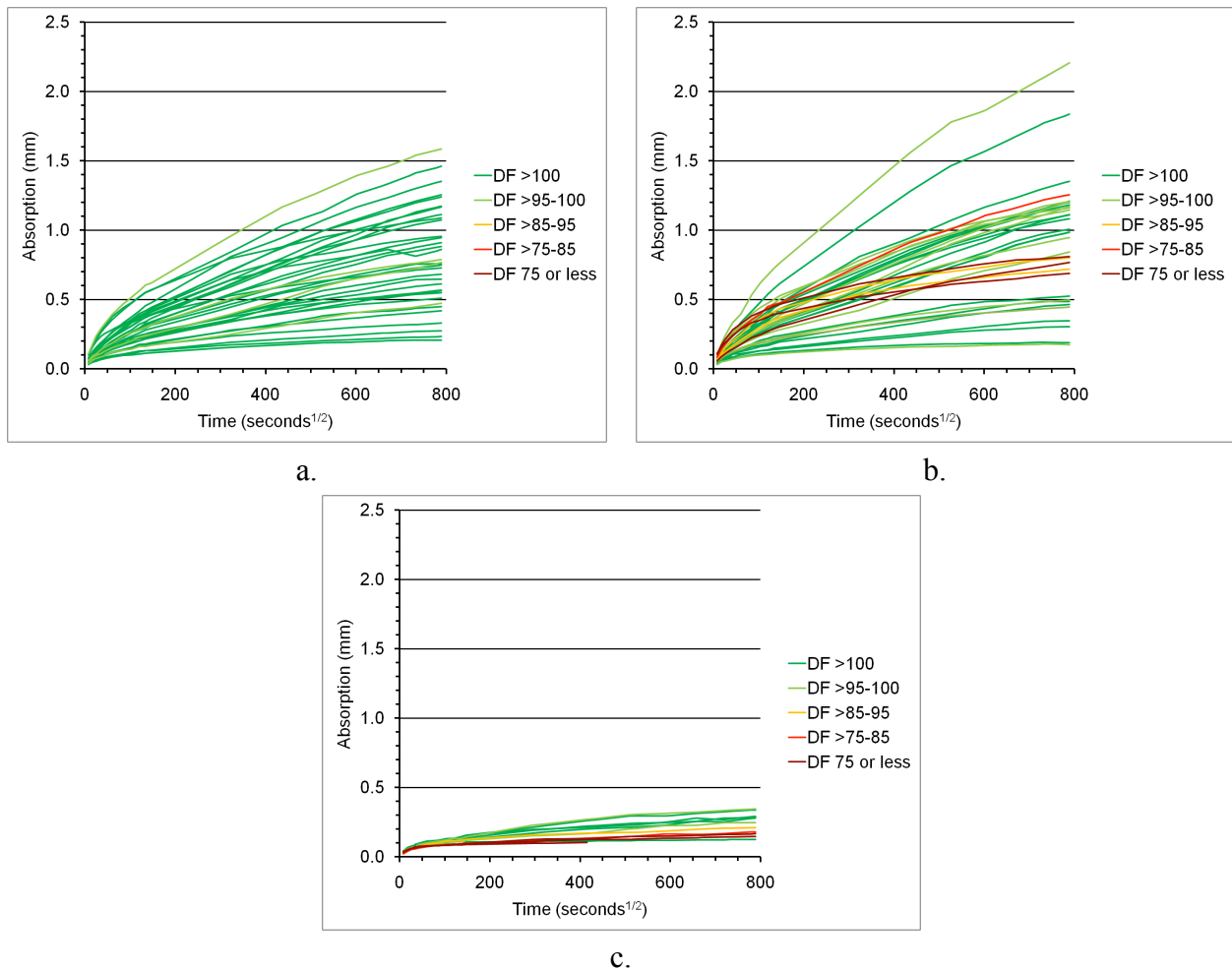


Figure 92: Absorptivity curves color-coded in terms of durability factor for (a) high target air content mixtures, (b) low air content target mixtures, and (c) very low air content target mixtures.

6.3.4 AEA Type and F-T Performance

Since so few mixtures performed poorly in F-T testing, it is difficult to draw any solid conclusions about the influence of AEA type, although of the concrete mixtures that failed in ASTM C666 Procedure B testing, four out of the five contained vinsol resin. Previous research by Tanesi and Meininger [2006] comparing the F-T performance of concrete produced with synthetic and vinsol resin based AEAs has indicated a tendency for higher specific surface values (smaller entrained air bubbles) for concrete produced with synthetic AEAs. To investigate this trend, Table 30 provides summary statistics for the specific surface values and void frequencies for chord lengths of less than 40 μm as measured by the flatbed scanner. A hypothesis test for two independent samples was performed to assess whether the frequency of average specific surface values and average void frequencies for the synthetic AEA mixtures were higher than those of the vinsol resin AEA mixtures at a significance level of 0.10 as listed below:

$$H_o: \mu_{syn} - \mu_{vinsol} = 0 \quad \text{Equation 6.5}$$

$$H_a: \mu_{syn} - \mu_{vinsol} > 0 \quad \text{Equation 6.6}$$

Where:

H_o = null hypothesis

H_a = alternative hypothesis

μ_{syn} = avg. synthetic AEA air-void parameter

μ_{vinsol} = avg. vinsol resin AEA air-void parameter

The critical value for the t statistic in all cases was determined at 1.308. For the specific surface values, as shown in Table 30, the critical value was only exceeded (and the null hypothesis rejected) for the high air content target mixtures. Thus, for the high air content target mixtures, the specific surface was significantly higher for the mixtures containing synthetic AEA. In all other cases the null hypothesis could not be rejected. For the void frequency of chord lengths less than 40 μm , the critical value was exceeded (and the null hypothesis rejected) for the high air content and low air content target mixtures. For the very low air content mixtures the null hypothesis could not be rejected. Thus, for the high air content and low air content target mixtures, the frequency of very short chord length intercepts was significantly higher for the mixtures containing synthetic AEA.

In conclusion, there is statistical evidence to suggest that concrete mixtures containing the synthetic AEA do yield greater numbers of smaller air-voids. Although there is a statistical difference, whether or not it is of practical significance is more difficult to determine. Figure 92 shows the same air-void chord length distribution plots of Figure 88, but color-coded according to AEA type. In Figure 93, a consistent trend for the frequency of small air-void chord length intercepts according to AEA type is difficult to discern.

Table 30: Summary statistics for air-void parameters as measured by flatbed scanner.

Target Air Content	AEA	# of Mixtures	Chord Intercept Lengths of <40 μm per m of traverse			Specific Surface (mm^{-1})		
			Avg.	Std. Dev.	Test Statistic	Avg.	Std. Dev.	Test Statistic
6.5 vol. %	Vinsol resin	18	1229.6	442.2	1.53	23.7	3.1	2.24
	Synthetic	16	1525.8	676.1		26.8	4.7	
3 vol. %	Vinsol Resin	18	531.3	115.6	1.51	16.3	3.9	-0.21
	Synthetic	16	621.1	221.5		16.1	2.8	
2 vol. %	Vinsol resin	6	326.7	114.7	0.97	0.1	0.0	-0.46
	Synthetic	6	392.8	121.3		0.1	0.1	

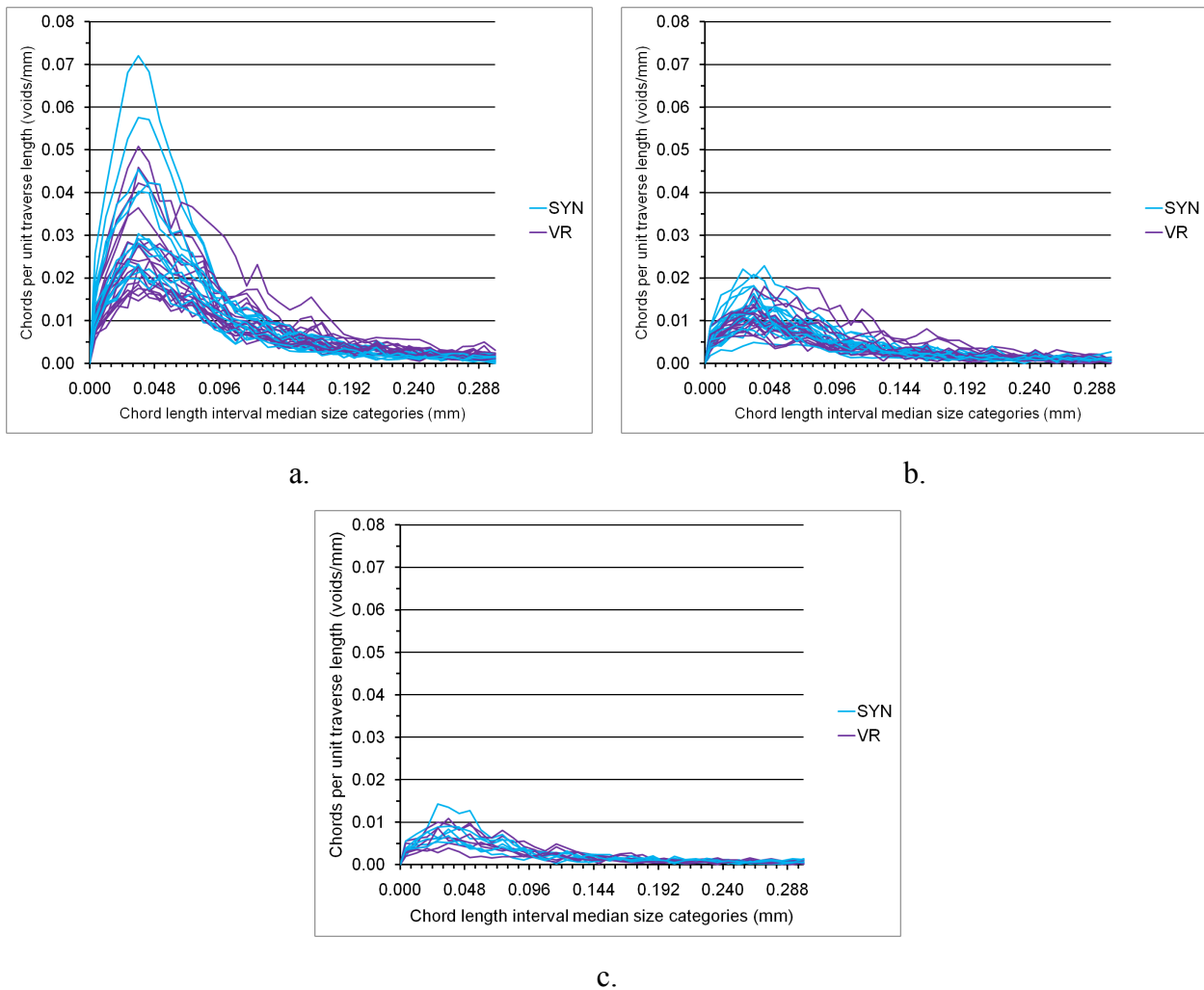


Figure 93: Chord length size distribution plots color-coded in terms of AEA type, (a) high target air content mixtures, (b) low air content target mixtures, and (c) very low air content target mixtures.

6.3.5 Duplicate Concrete Mixtures that Exhibited Variable F-T Performance

As shown in Figure 31 and Table 8, one of the LO-VR-SLG-5SK-45WC mixtures performed well in F-T testing (a durability factor of 100) while the duplicate mixture performed poorly (a durability factor of 50). Section 5.2.5 contains the fluorescence measurements from thin sections prepared these mixtures, with Figure 55 and Table 23 summarizing the results from the good F-T performance mixture, and Figure 56 and Table 24 summarizing the results from the poor F-T performance mixture. Both mixtures had a dense paste microstructure, with equivalent w/cm values of 0.29 and 0.32 for the good and poor mixtures respectively. Although the paste densities were similar, and similar in appearance, as shown in Figures 55 and 56, there was a contrast in the fresh concrete test results of Table 5, as the poor F-T performance mixture had a 0.00 inch slump, while the good F-T performance mixture had a 0.75 inch slump. As mentioned in Sections 6.2.1 and 6.2.2, the zero-slump mixture was difficult to consolidate, which may have played a role in its poor F-T performance. The pressure meter tests also showed less air in the poor F-T performance mixture (2.2 vs. 3.4 vol. % air) and this was also reflected in the flatbed scanner spacing factor measurements (0.291 vs. 0.236 mm). The contrast in performance between the LO-VR-SLG-5SK-45WC mixtures can be attributed to problems with consolidation, and the less-than-ideal air-void parameters for the poor F-T performance mixture.

A similar scenario was played out for the LO-SYN-FA-6SK-45WC mixtures, as shown in Figure 30 and Table 8, where the good F-T performance mixture had a durability factor of 97, and the poor F-T performance mixture had a durability factor of 81. Again, the fluorescence measurements from Section 5.2.5 show similar equivalent w/cm values (0.47 and 0.48 equivalent w/cm for the good and poor mixtures respectively), as summarized in Figures 57 and 58, and in Tables 25 and 26. The fresh concrete test results listed in Table 5 were also very similar; for the good and poor mixtures the slumps were 2.25 inch and 2.5 inch respectively, the pressure meter air contents were 3.4 and 3.5 vol. % respectively, and the flatbed scanner spacing factors were 0.240 and 0.260 mm respectively. With such similar characteristics, it would be expected for the mixtures to behave identically. However, a careful examination of Figure 30 shows that although the “good” F-T performance mixture did have a durability factor of 97 at 300 cycles, it does appear that the mixture was at the beginning of a downward trend in RDME not unlike its poor F-T performance companion mixture.

6.3.6 Insights from CEMHYD3D Modeling to F-T Performance

In this study, CEMHYD3D was used only to model various w/cm scenarios for a 100% portland cement system. The model can also be used to model the hydration of portland cement and SCM systems, but requires detailed characterization of the SCMs similar to that described in Section 5.2.6 for the characterization of the portland cement. The model showed the expected pattern of increased porosity for the hydrated systems at elevated w/cm values as shown in Figure 70. The model also predicted the discontinuity of the pore system over a scale of 0.1 mm for the 0.45 w/cm at 40 days, as shown in Figure 71. This value of 0.1 mm also approximated the Philleo factor threshold above which reductions in the ASTM C666 Procedure B durability factor

become more frequent. The Philleo factor defines the distance at which 90% of the hardened cement paste is within an air void. Therefore, it would be likely that a $0.1 \times 0.1 \times 0.1$ mm cube of hardened cement paste from a concrete with a measured Philleo factor of less than 0.1 mm would contain an air void, or portion thereof. Presumably, the presence of an entrained air-void within the modeled $0.1 \times 0.1 \times 0.1$ mm cube would restore the connectivity of pore system for the 25-day 0.45 *w/cm* scenario. Although not modeled in this study, CEMHYD3D has the capability of introducing a flat surface in order to simulate variations in microstructure that may occur at an aggregate interface, and could possibly be modified to allow the introduction of an entrained air void. The concept of a pessimum porosity as discussed in Section 6.3.3, for which the degree of interconnectivity of the pores may influence the F-T durability, could be explored further within the context of the CEMHYD3D model. Figures 72-73, comparing model output to actual hydrated microstructure, show many similarities, although it is clear that the model does not encompass the finer details of the microstructure due to the limited $1 \mu\text{m}^3$ voxel resolution.

6.4 Mixtures Exhibiting Delayed Set

As previously discussed in Sections 5.1.3 and 6.1.1. the LO-SYN-SLG-6SK-45WC mixtures experienced a delay in set. Other mixtures performed at similar or higher temperatures with the same combination and similar dosage of admixtures but without slag cement did not exhibit a delay in set. A complex interaction between temperature, synthetic AEA, water reducing admixture, and the presence of slag cement may have led to the delay in set. However, other irregularities in the development of the heat curves were also observed in the LO-VR-SLG-5SK-45WC mixtures (equivalent vinsol resin AEA mixtures) that also occurred at relatively higher temperatures as shown in the heat curve of Figure 15. Although delayed set did not occur for the LO-VR-SLG-5SK-45WC mixtures, a double peak occurred in the heat curve, with the first peak at about 16 hours, and the second peak at about 27 hours. So, it is possible that the delayed set may be a combination of elevated temperature, the presence of slag cement, and chemical admixtures used in the mixture (i.e. type of AEA and water reducer). Repeat trials of the LO-SYN-SLG-6SK-45WC mixture performed at a variety of lower and higher temperatures did not experience the same delayed set, as discussed in Section 5.1.3.

A review of unusual admixture/SCM interactions by Roberts and Taylor [2007] discusses the role of sulfate ions as related to occurrences of delayed set. Sources of calcium sulfate are usually interground with cement clinker during the production of portland cement. The role of the sulfate is to suppress the rapid hydration of the aluminate phases present in cement clinker, and prevent what is commonly referred to as flash set. In SCM systems where additional sources of aluminate are present, beyond that of the portland cement, situations may occur where there is insufficient sulfate present to control the hydration of the aluminate phases. Rapid hydration of the aluminate phases consumes calcium ions that would otherwise contribute to the hydration of the silicate phases necessary for normal strength gain, leading to delayed set. The presence of admixtures may further exacerbate the situation through increased dispersion of particles and increased reactive surface area for the aluminate phases. Similarly, elevated temperature may

increase the reactivity of the aluminate phases. In such situations, providing additional sources of sulfate may prevent delayed set. Because the specific conditions leading to the delayed set mixture observed in the laboratory could not be identified and reproduced, the possibility of exploring the utility of sulfate additions could not be undertaken in this study.

In spite of the delay in set, the LO-SYN-SLG-6SK-45WC mixtures did achieve the required 2,600 psi at 7 days as listed in Table 8, with compressive strengths of 7,128 and 5,501 psi for the duplicate mixtures, and both mixtures also performed well in F-T with durability factors of 96 and 99. The fluorescence measurements from Section 5.2.5 comparing the delayed set mixture to its vinsol resin counterpart (LO-VR-SLG-6SK-45WC), as summarized in Figures 59 and 60, and in Tables 27 and 28, also show similar values for paste density, with equivalent w/cm values of 0.33 and 0.34 for the delayed set and normal set mixtures respectively.

7. Conclusions

Overall, modern cements and the use of SCMs lead to a hardened cement paste that can potentially have a higher tensile strength and lower permeability. Current limits on both total air content and air void system parameters were established many years ago with different cements, different admixtures, and limited use of SCMs. Evidence indicates that these traditional limits should provide a conservative estimate of performance and incorporating SCMs into concrete mixtures does not necessarily require deviation from these traditional air-void system thresholds. The production of paving concretes with reduced CMC has become more common, and the durability of these concretes, in terms of the laboratory ASTM C666 testing conducted in this study, is superior to the traditional 564 lbs/yd³ CMC concrete, especially for concrete that falls below the 6.5 ± 1.5 vol. % total air content as reported using standard field measurement equipment. The ASTM C666 Procedure B test regime of freezing in air did not adversely affect the concrete mixtures with elevated w/cm values of 0.50 and 0.52. However, all the variations on the ASTM C666 Procedure A test regime (i.e. freeze in water, freeze in 4.0 wt. % CaCl₂ brine, and freeze in 4.2 wt. % NaCl brine) were found to be similarly more aggressive with increased scaling, and rapidly caused the failure of the 0.50 and 0.52 w/cm concrete mixtures.

There is general agreement between methods of measuring the total air content of a concrete mixture using conventional field testing methods (i.e. ASTM C231 and ASTM C173). However, the AVA, a non-standard test, generally does not perform well for this task. Considering the amount of labor involved in the cutting and polishing of hardened concrete samples for air-void analysis, the flatbed scanner method may not be a practical choice for air content determination of field concretes, although other states and provinces have developed specifications that do use ASTM C457 measurements as a pay factor adjustment (e.g. Pennsylvania and Ontario). Also, alternative approaches should be studied further. As an example, even without detailed measurements of the air void size distribution, the pressure meter air content results and paste content estimates (as computed from the mix design, and defined as the total concrete volume minus the aggregate volume and the air content) appear to perform just as well as the spacing factor calculation at predicting F-T performance.

With current admixtures, concrete produced with the currently specified level of total air content (e.g. 6.5 ± 1.5 vol. %) can be expected to be F-T durable. Likewise, the current demarcation of an air-void system spacing factor less than or equal to 0.2 mm is still a safe value to ensure F-T durability. It is the recommendation of the research team that these two current measures of air-void system adequacy, with respect to F-T durability, continue to be employed. The research presented here clearly shows these values to be prudent.

It should be noted, as an item of further research, that concrete produced with a total air content lower than 6.5 ± 1.5 vol. % or with a spacing factor greater than 0.2 mm can also be F-T durable. However, this is not universally true. There is evidence in this study that concrete produced using an SCM, and having a low air content, is less resistant to freeze-thaw damage than a comparable mix with no SCM. Also it is noteworthy that all concretes mixtures produced with 6.5 ± 1.5 vol. % target air, with or without inclusion of an SCM, were freeze-thaw resistant. Therefore, before changes in the current air content specification can be recommended, additional information regarding mixtures with air-void system parameters now considered marginal must be obtained.

Test results for water content by the microwave oven drying test method compared well with the mixture designs. Test results for w/cm by the Cementometer™ were not as promising, but may be improved with further attention to the calibration process. The petrographic fluorescent method of w/cm determination followed general trends of increased fluorescence intensity with increased w/cm , but exhibited a wide scatter on individual thin sections ($\pm 0.05 w/cm$) and would require standards with similar curing regimes and SCM content for more accurate w/cm determinations.

Semi-adiabatic calorimetry proved to be useful tool for identifying delayed-set mixtures. Detecting the delay of initial set, a precursor to delaying the final set, can provide critical information to field personnel regarding issues associated with a particular set of conditions for that concrete mixture and placement. Even if the exact cause is unknown, the additional hours of advanced warning can eliminate the cost of placing material that may subsequently need to be removed.

8. Recommendations for Implementation & Further Research

Based on the research presented, the following general recommendations are made for implementation.

- Increase the use of reduced CMC mixtures (i.e. $< 564 \text{ lbs/yd}^3$ CMC mixtures) accomplished in conjunction with use of an optimized aggregate gradation in the concrete mixtures. It is not recommended to reduce CMC without optimizing the aggregate gradation.
- Continue the use of fly ash and slag cement mixtures.
- Maintain the current air content specification (i.e. $6.5 \pm 1.5 \text{ vol. } \%$).
- This research did not investigate the performance of concrete mixtures with total air contents greater than $6.5 \pm 1.5 \text{ vol. } \%$. However, given the observed performance of concrete with total air contents of $6.5 \pm 1.5 \text{ vol. } \%$, there does not appear to be any justification for increasing the air content specification beyond this level.
- The AVA should not be used for determining total air content in the field. It could possibly have use as a quality control method for assessing air-void system parameters. Before adopting the AVA for this purpose, a more rigorous examination of this technique is required.
- Consider the use of AASHTO T 318 with a correction for aggregate absorption as a quality control technique. Based upon the research presented here, ASTM is currently balloting a version of the microwave water content test that includes a correction for aggregate absorption.
- Caution should be exercised in using SCMs, AEAs, and other chemical admixtures in combinations that have not been fully tested in the field. These variables, in combination with placement temperature, can lead to delayed setting times.

Based on the research presented, the following general recommendations are made for future research.

- Based upon a fixed, specified CMC (i.e. 5 sack or 5.5 sack), examine a broader matrix of synthetic AEAs to determine if lower total air contents can be safely specified with synthetic AEAs. Preliminary evidence, for one synthetic AEA, indicates a higher number of air voids (i.e. a smaller spacing factor) for air-void systems in concrete prepared using that AEA.
- Develop a methodology for the use of paste content as a variable when specifying air-void systems given that a significant relationship between paste content, air content, and F-T performance was observed
- Explore alternative means for characterization of the capillary porosity in HCP in terms of F-T performance (e.g. mercury porosimetry).
- Perform a characterization of fly ash and slag for input into CEMHYD3D model and for generation of hydrated systems incorporating air voids to model their influence on pore interconnectivity. In addition, hydrated models may possibly be used as a starting-point for finite element modeling of the impact of freezing water in pore systems.

9. List of Acronyms, Abbreviations and Symbols

AEA	Air entraining admixture
ASTM	American Society for Testing and Materials
BSE	Back-scattered electron
C ₃ S	Alite or Tricalcium Silicate
C ₂ S	Belite or Dicalcium Silicate
C ₃ A	Aluminate or Tricalcium aluminate
C ₄ AF	Ferrite or Tetracalcium aluminoferrite
CMC	Cementitious material content
EDS	X-ray energy dispersive spectroscopy
F-T	Freeze-thaw
HCP	Hydrated cement paste
MDOT	Michigan Department of Transportation
Na ₂ O _{equiv.}	The equivalent wt. % of Na ₂ O that would yield the same moles of alkalis as the sum of the wt. % Na ₂ O and K ₂ O in the cement.
NIST	National Institute of Standards and Technology
RDME	Relative dynamic modulus of elasticity
SCM	Supplementary cementitious material
SEM	Scanning electron microscope
w/cm	Water to cementitious material ratio, by weight.

10. References

- AASHTO T 318-02, "Standard Method of Test for Water Content of Freshly Mixed Concrete Using Microwave Oven Drying," American Association of State Highway and Transportation Officials, Washington, D.C., (2002).
- ASTM C39/C39M-10, "Standard Test Method for Compressive Strength of Cylindrical Concrete Specimens," American Society for Testing and Materials, West Conshohocken PA, (2010).
- ASTM C114-10a, "Standard Test Methods for Chemical Analysis of Hydraulic Cement," American Society for Testing and Materials, West Conshohocken PA, (2010).
- ASTM C138/C138M-10b, "Standard Test Method for Density (Unit Weight), Yield, and Air Content (Gravimetric) of Concrete," American Society for Testing and Materials, West Conshohocken PA, (2010).
- ASTM C143/C143M-10a, "Standard Test Method for Slump of Hydraulic-Cement Concrete," American Society for Testing and Materials, West Conshohocken PA, (2010).
- ASTM C173/C173M-10b, "Standard Test Method for Air Content of Freshly Mixed Concrete by the Volumetric Method," American Society for Testing and Materials, West Conshohocken PA, (2010).
- ASTM C231/C231M-10, "Standard Test Method for Air Content of Freshly Mixed Concrete by the Pressure Method," American Society for Testing and Materials, West Conshohocken PA, (2010).
- ASTM C457/C457M-10a, "Standard Test Method for Microscopical Determination of Parameters of the Air-Void System in Hardened Concrete," American Society for Testing and Materials, West Conshohocken PA, (2010).
- ASTM C666/C666M-03(2008), "Standard Test Method for Resistance of Concrete to Rapid Freezing and Thawing," American Society for Testing and Materials, West Conshohocken PA, (2008).
- ASTM C1064/C1064M-08, "Standard Test Method for Temperature of Freshly Mixed Hydraulic-Cement Concrete," American Society for Testing and Materials, West Conshohocken PA, (2008).
- ASTM C1074-10, "Standard Practice for Estimating Concrete Strength by the Maturity Method," American Society for Testing and Materials, West Conshohocken PA, (2010).
- ASTM C1585-04e1, "Standard Test Method for Measurement of Rate of Absorption of Water by Hydraulic-Cement Concretes," American Society for Testing and Materials, West Conshohocken PA, (2004).
- ASTM C856-04, "Standard Practice for Petrographic Examination of Hardened Concrete," American Society for Testing and Materials, West Conshohocken PA, (2004).

American Concrete Institute Committee 201, (2008), Guide to Durable Concrete, ACI Manual of Concrete Practice, ACI 201.2R-08, American Concrete Institute, Farmington Hills, MI.

Bentz D.P., (2005), CEMHYD3D: A Three-Dimensional Cement Hydration and Microstructure Development Modeling Package. Version 3.0, NISTIR 72132, National Institute of Standards and Technology, Technology Department Administration, U.S. Department of Commerce, Gaithersburg, MD. <http://ciks.cbt.nist.gov/~garbocz/monograph/appendix2.html>

ImageJ, (2010), A Public Domain Java Image Processing Program, <http://rsbweb.nih.gov/ij/index.html>

Elsen J., Lens N., Aarre T., Quenard D., Smolej V., (1995), "Determination of the w/c Ratio of Hardened Cement paste and Concrete Samples on Thin Sections Using Automated Image Analysis Techniques" *Cement and Concrete Research*, Vol. 25, No. 4, pp. 827-834.

MultiSpec ©, (2010) A Freeware Multispectral Image Data Analysis System, <https://engineering.purdue.edu/~biehl/MultiSpec/>

Peterson K., Sutter L., Radlinski M., (2009) "The Practical Application of a Flatbed Scanner for Air-Void Characterization of Hardened Concrete," *Journal of ASTM International*, Vol. 6, No. 9, 15 p., 2009.

Philleo R.E., (1983), "A Method for Analyzing Void Distribution in Air-Entrained Concrete," *Cement, Concrete, and Aggregates*, Vol. 5, No. 2, pp. 128-130.

Roberts L., Taylor P., (2007), "Understanding Cement-SCM-Admixture Interaction Issues," *Concrete International*, Vol. 29, Issue 1, pp. 33-41.

Shilstone, J., "Concrete Mixture Optimization," *Concrete International*, American Concrete Inst., Farmington Hills, Michigan, USA, June 1990, Vol. 12, No. 6, pp. 33-39.

Snyder K., Natesaiyer K., Hover K., (2001), "The Stereological and Statistical Properties of Entrained Air-Voids in Concrete: A Mathematical Basis for Air-Void System Characterization," Materials Science of Concrete VI, Mindess S., Skalny J., (Eds.) American Ceramic Society, pp. 129-214.

Tanesi J., Meininger R., (2006), "Freeze-Thaw Resistance of Concrete With Marginal Air Content" FHWA-HRT-06-117, Federal Highway Administration, McLean, VA, 93 p. <http://www.fhwa.dot.gov/pavement/pccp/pubs/06117/index.cfm#toc>

Tazawa E., Miayazawa S., Kasai T., (1995), "Chemical Shrinkage and Autogenous Shrinkage of Hydrating Cement Paste," *Cement and Concrete Research*, Vol. 25, pp. 288–29.

Thaulow N., (2002), "Identification of Phases in Cement and Concrete Using Backscattered Electron Imaging," *Proceedings of the Twenty-fourth International Conference on Cement Microscopy*, International Cement Microscopy Association, April 7-11, San Diego, CA, pp. 214-223.